**PROLONGED ROUGHNESS AT SIMPLE LUNAR IMPACT CRATER RIMS.** C. A. Nypaver[1], B. J. Thomson[1], M. McCanta[1], G. W. Patterson[2], J.T. Cahill[2], S. S. Bhiravarasu[3]. [1]The University of Tennessee, Knoxville. 1621 Cumberland Ave, 602 Strong Hall, Knoxville, TN 37996 (cnypaver@vols.utk.edu). [2]Applied Physics Laboratory, Johns Hopkins University, Baltimore, MD 21218. [3]Lunar and Planetary Institute, Houston, TX 77058.

**Introduction:** Over time, rocks at the lunar surface breakdown due to space weathering processes such as micrometeoroid bombardment and thermal cycling [1–2]. Models of this breakdown process predict that 99% of boulders exposed at the surface of lunar impact ejecta deposits should be completely destroyed on timescales of 150–300 Ma [e.g., 3]. However, we observed large (>2 m–diameter) boulders present at the rims of old (>3.0 Ga) simple impact craters on the lunar maria (Fig. 1). This observation of intact boulders on old crater rims is inconsistent with prior models of lunar boulder breakdown and potentially indicates that these boulders are being exhumed, uncovered, or transported by geologic processes that are currently unrecognized. The goal of this work is to constrain the mechanisms responsible for the prolonged presence of boulders at simple crater rims and compare the roughness at crater rims with that of crater ejecta over time. Our working hypothesis for this project is that intact boulders are being uncovered at crater rims due to the downslope motion of the overlying regolith at a rate that exceeds that rate of boulder breakdown on the Moon.

**Background:** Ejecta deposits on the lunar surface are poorly sorted mixtures of fine-grained regolith, cobbles, and large boulders that are ejected from an impact crater upon formation [e.g., 4]. In cases of impacts within 45° of vertical, ejecta constituents are deposited radially in all directions from the central crater with larger rocks and boulders concentrated near the crater rim [5]. In this study, the roughness associated with these lunar ejecta deposits is measured using Lunar Reconnaissance Orbiter (LRO) Mini-RF monostatic S-band (12.6 cm wavelength) circular polarization ratio (CPR) data [6] and Diviner rock abundance (RA) data [7]. These data provide complimentary measurements of roughness in that CPR is sensitive to lunar rocks at the centimeter-meter scale at the lunar surface and subsurface while RA data are sensitive to rocks >1 m at the lunar surface only.

Ages for all craters analyzed here are derived from topographic degradation state in a prior study [8]. That study showed that, over time, simple lunar impact craters <5 km in diameter infill with regolith and their once-sharp rim crests become rounded. The rate at which this degradation process occurs is heavily based on crater size, however, and craters in the diameter range examined here (0.8–2.0 km) exhibit the most clear rates of degradation.

**Methods:** We utilize a sample set of 6087 craters on the lunar maria, all of which possess model ages from [8]. Those model ages were obtained by, first, extracting real topographic profiles for all craters in question. The hillslope diffusion equation was then used to forward model the degradation process for a symmetrical simple lunar crater, and the real topographic profiles were fit to this model to obtain degradation values for each crater with the units $\kappa t$, where $\kappa$ represents diffusivity and $t$ represents time in Ga. The size-frequency distributions of craters surrounding each study crater were then fit to the Neukum production function [9] to link degradation state and age. All crater center points were loaded into ArcMap 10.6 as a single shapefile overlaid onto the RA and CPR global mosaics. Individual polygons were drawn over the crater interiors (0–1.0 crater radii), the crater rims (1–1.5 crater radii), and the distal ejecta (1.5–4.0 crater radii). The ArcMap Zonal Statistics tool was used to average and extract all CPR and RA data values under each polygon. Lastly, the mean CPR and RA values for the crater rims and ejecta were binned in 1000 $\kappa t$ increments to create 30 bins of ~50–300 craters each.

**Results:** A comparison of RA and CPR data for crater rims and ejecta (Fig. 2) indicates that the RA data associated with crater rims is elevated above that of the ejecta at the beginning of the craters' lifetime (Fig. 2a) and may remain elevated for the lifetime of all craters in our dataset. This dichotomy between crater rim and ejecta data is more evident in RA than CPR, but it is worth noting that both datasets associated with ejecta reach background values in ~13,000–14,000 $\kappa t$ (~2.0 Ga). This ejecta–rim dichotomy is slightly less apparent in CPR data where average crater rim CPR values fall only slightly above average ejecta values (Fig. 2b), but these differences are well within error of one-another for every sample bin. Lastly, a comparison of rims and ejecta deposits for three individual craters in Mini-RF bistatic data indicates that those data follow similar evolutionary trends (albeit with systematically lower values) to the data in monostatic images. Therefore, this analysis appears broadly reproduceable using Mini-RF bistatic data which is more geospatially controlled with higher signal to noise [10].

**Discussion:** The differences in roughness data values for crater rims and ejecta indicate that a potential dichotomy exists between the quantity of boulders

present on crater rims and ejecta blankets generated over extended periods of time. Roughness data associated with ejecta blankets go to background values of CPR and RA within ~2.0 Ga. This result is broadly consistent with prior characterizations of lunar ejecta using these data [11-12]. Contrary to the roughness of ejecta deposits, boulders appear to be present at the summit of crater rims for 2.5–3.7 Ga aged craters. This finding is in disagreement with prior work showing that boulders on the lunar surface break down relatively quickly [e.g., 3].

One possible explanation for our observations of elevated crater rim roughness is that boulders or partially fragmented bedrock are continually being exposed at crater rims due to the downslope motion of the overlying regolith. A continual uncovering of boulders or fragmented/fractured bedrock implies that crater rims are localities on the lunar surface where rocks are more likely to be 'in-situ', providing a valuable target for future lunar sample return missions. Moreover, this regional difference in CPR and RA should be taken into account for characterizations of impact ejecta roughness or systematic degradation.

**Future work:** A more extensive analysis of these craters in LROC NAC images is currently underway to further investigate this dichotomy in crater rim-ejecta roughness. Moreover, a comparison of craters in Mini-RF bistatic S and X-band data is likely to reveal the presence of any grain size differences that exist between crater rims and ejecta deposits.

**References:** [1] Ross H. P. (1968) *J. Geophys. Res.*, 73, 1343–1354 [2] Soderblom, L. A. (1970) *Nature*, 538, 215. [3] Basilevsky A. T. et al. (2013) *Planetary and Space Sci., 89, 118–126.* [4] Koeberl C. (2013) *Encyc. of Natl. Haz., 18–28* [5] Bart G. D. and Melosh H. J. (2007) *Geophys. Res. Lett.*, 34 [6] Raney R. K. et al., (2011) *Proc. IEEE*, 99, 808–823 [7] Bandfield J. L. et al., (2011) *J. Geophys. Res.*, 116, E00H02 8 [8] Fassett C. I. and Thomson B. J. (2014) *J. Geophys. Res., 119*, 2255–227 [9] Neukum G. et al., (2001) *Space Sci. Revs.* 96, 55. [10] Patterson G. W. et al., (2017) *Icarus*, 283, 2–19 [11] Ghent et al., (2016) Icarus, 273, 182–195 [12] Saran et al., (2014) Adv. in Space. Sci, 2101-2113.

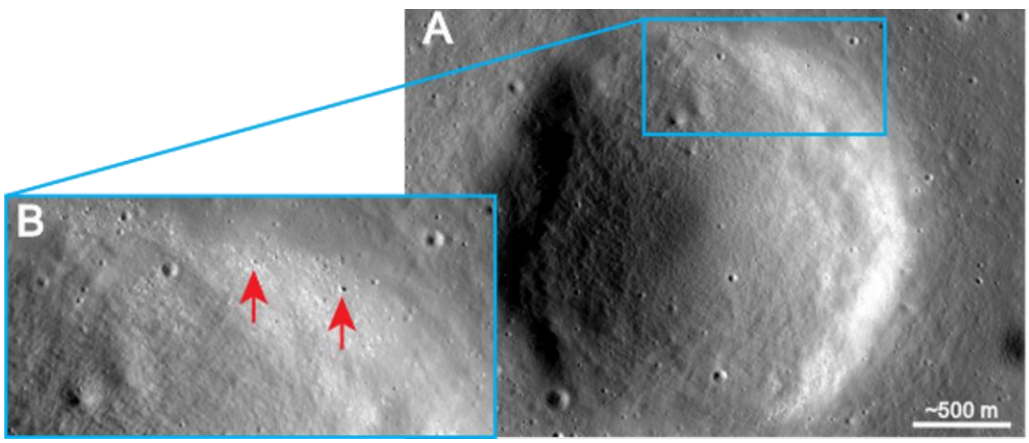


**Figure 1:** (A) LROC NAC image of a simple crater (UniqID: 5157) on Mare Nubium (-20.206° S, -9.031° W) with a modelled age of ~3.7 Ga (*κt*: 26203). (B) Enhanced image of the NE portion of the crater rim with red arrows indicating two of the larger boulders present in this region.

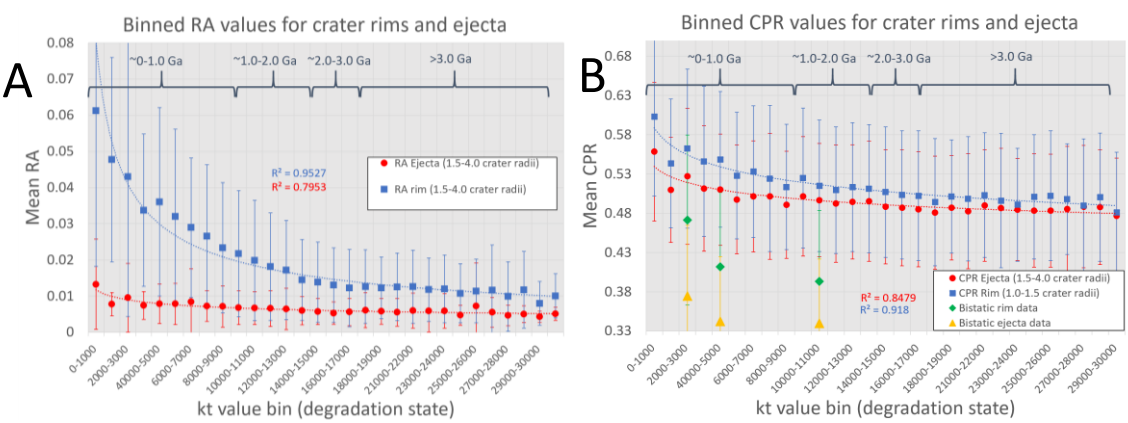


**Figure 2:** Binned evolution of CPR (A) and RA (B) values associated with the crater rim region (blue squares) and ejecta (red circles). Green, diamond shaped data points represent crater rims and yellow triangles represent crater rims ejecta in Mini-RF bistatic data as opposed to monostatic data.